



# The plant cytoskeleton controls regulatory volume increase

Qiong Liu<sup>a</sup>, Fei Qiao<sup>b,\*</sup>, Ahmed Ismail<sup>a</sup>, Xiaoli Chang<sup>a</sup>, Peter Nick<sup>a</sup>

<sup>a</sup> Molecular Cell Biology, Botanical Institute, Karlsruhe Institute of Technology, Kaiserstr. 2, 76128 Karlsruhe, Germany

<sup>b</sup> Tropical Crops Genetic Resources Institute, Chinese Academy of Tropical Agricultural Sciences/Key Laboratory of Crop Gene Resources and Germplasm Enhancement in Southern China, Danzhou City, Hainan Province, 571737, China

## ARTICLE INFO

### Article history:

Received 27 March 2013

Received in revised form 28 April 2013

Accepted 30 April 2013

Available online 6 May 2013

### Keywords:

Cytoskeleton

Protoplast

Osmotic expansion

Vitis

Regulatory cell volume control

## ABSTRACT

The ability to adjust cell volume is required for the adaptation to osmotic stress. Plant protoplasts can swell within seconds in response to hypoosmotic shock suggesting that membrane material is released from internal stores. Since the stability of plant membranes depends on submembraneous actin, we asked, whether this regulatory volume control depends on the cytoskeleton. As system we used two cell lines from grapevine which differ in their osmotic tolerance and observed that the cytoskeleton responded differently in these two cell lines. To quantify the ability for regulatory volume control, we used hydraulic conductivity ( $L_p$ ) as readout and demonstrated a role of the cytoskeleton in protoplast swelling. Chelation of calcium, inhibition of calcium channels, or manipulation of membrane fluidity, did not significantly alter  $L_p$ , whereas direct manipulation of the cytoskeleton via specific chemical reagents, or indirectly, through the bacterial elicitor Harpin or activation of phospholipase D, was effective. By optochemical engineering of actin using a caged form of the phytohormone auxin we can break the symmetry of actin organisation resulting in a localised deformation of cell shape indicative of a locally increased  $L_p$ . We interpret our findings in terms of a model, where the submembraneous cytoskeleton controls the release of intracellular membrane stores during regulatory volume change.

© 2013 Elsevier B.V. All rights reserved.

## 1. Introduction

Life requires that an internal space is chemically differentiated from the environment. The goal is achieved by semipermeable biomembranes therefore are subjected to osmotic challenges. In multicellular animals cells are protected from osmotic challenges by excretion organs that establish an isotonic cellular environment. This strategy is not possible for bacteria, fungi, and plants that have to cope with strong variations of osmotic conditions. Upon sufficient supply with water, the cell membrane of these organisms experiences considerable pressure from the cell interior against the resistance of the cell wall. In contrast, when these cells are exposed to extreme hyperosmotic stress or high salinity, especially outside a tissue context, the protoplast shrinks and can even detach from the cell wall. In order to maintain a functional metabolism, the cells must be able to sense osmotic changes and to adjust their volume correspondingly. It is therefore not surprising that already prokaryotes have evolved mechanisms to sense osmotic forces at the plasma membrane (reviewed in [1]). Osmosensing is then followed by active changes in volume (reviewed in [2]). Already several decades ago, wall-free plant protoplasts were shown to swell or shrink

considerably within seconds in response to fluctuations of osmotic potential without losing their spherical shape [3]. Osmotic swelling or shrinkage of spherical protoplasts proceed within a couple of minutes, and must therefore be caused either by insertion of additional membrane material (in case of swelling) or by internalisation of excess membrane material (in case of shrinking) [3–5]. This rapid osmotic swelling differs from the slow swelling reported for protoplasts generated from guard cells in response to blue light that requires 1 to 2 h and probably involves gene regulation [6]. The situation in osmotically challenged plant protoplasts is different from that in animal cells, where large proportions of the cell membrane are folded into filopodia, ruffles, and other protrusions, such that considerable increases in cell volume can be accommodated without the need for adjusting the cell surface (reviewed in [7]).

Prokaryotes respond to osmotic stress by active transport of ions as shown for the mechanosensitive channel of large conductance, MscL, in *E. coli* [1]. In animal cells, such concentration changes remain minute [7], and are therefore thought to be of minor impact as compared to the yielding of membrane protrusions and ruffles. Since animal cells lack cell wall and the plasma membrane itself cannot provide a mechanical barrier, the actin cytoskeleton has been proposed to be involved in the mechanism that allows shape control after osmotic challenges [2,7,8]. In plant cells as well, a hyperosmotic shock was shown to cause bundling of actin [9] and microtubules [10], indicating a connection between cytoskeleton and membrane tension.

In our previous work we have shown for tobacco BY-2 cells that stabilisation of actin by either phalloidin [11], or by inducible expression

Abbreviations:  $L_p$ , hydraulic conductivity

\* Corresponding author at: Tropical Crops Genetic Resources Institute, Chinese Academy of Tropical Agricultural Sciences, Danzhou, Hainan, China. Tel.: +86 898 2330 6675.

E-mail addresses: [liuqiongl@mail.com](mailto:liuqiongl@mail.com) (Q. Liu), [qiaofeixn@gmail.com](mailto:qiaofeixn@gmail.com) (F. Qiao), [ahmedaalkarim@yahoo.com](mailto:ahmedaalkarim@yahoo.com) (A. Ismail), [xl.changkit@hotmail.com](mailto:xl.changkit@hotmail.com) (X. Chang), [peter.nick@kit.edu](mailto:peter.nick@kit.edu) (P. Nick).

of an actin-bundling domain [12] also stabilised the plasma membrane against electric permeabilisation. By total internal reflection fluorescence microscopy (TIRF), we were able to visualise a subset of the cytoskeleton that was directly adjacent to the plasma membrane. Stabilisation of the submembraneous cytoskeleton caused an increase in the apparent thickness of the cell membrane. Since the elementary membrane cannot be resolved by light microscopy, these changes of apparent thickness must be caused by membrane topologies, leading to a model of tubulovesicular membrane folds or invaginations that increase membrane surface and might be structurally maintained by actin filaments [12].

This model predicts that the swelling response of protoplasts which are subjected to a hypoosmotic shock should depend on the status of the submembraneous cytoskeleton. The permeability of the membrane to water is conventionally described as hydraulic conductivity ( $L_p$ ) used as indicator for membrane behaviour. The permeability of the membrane to water has been successfully used to quantify the activity of aquaporins [13]. A variation of this approach used osmolytes with variable hydrodynamic radii to estimate the size of the pores induced by nanosecond pulsed electrical fields (nsPEFs) [14]. When the cytoskeleton participates in volume control by regulating the insertion or release of submembraneous resources of membrane material, pharmacological manipulation of the cytoskeleton should result in changes of  $L_p$ . In fact, more than two decades ago, water permeability in the two poles of internodal cells in Characean algae had been reported to depend differentially on actin [15]. In these giant cells that often are 100 mm in length, actin is organised into prominent cortical bundles driving the rapid cytoplasmic streaming essential to provide nutrient transport. Whether this phenomenon is specific for this peculiar and highly specific cell type, or whether it is general for cells from higher plants, has remained unclear.

The North American grape *Vitis rupestris* inhabits sunny rocks and slopes and is therefore used in viticulture as drought-tolerant rootstock. In contrast, the North American *Vitis riparia*, growing in alluvial forests, is less adapted to drought. We have shown previously [16] that a cell line derived from *V. rupestris* is more salt tolerant as compared to a cell line derived from *V. riparia* and that this difference in salt tolerance is located in the early steps of signalling upstream of jasmonate. In fact, *V. riparia* can be rescued to the level observed in *V. rupestris*, when it is supplemented with exogenous jasmonate. In the current work, we therefore use these two grapevine cell lines to probe for the role of the submembraneous cytoskeleton using  $L_p$  as indicator for the status of the cytoskeleton. To test the influence of actin organisation on membrane geometry directly, we used optochemical engineering of actin organisation as strategy. The plant hormone indolyl-3-acetic acid (an inducer of actin dynamicity) was released from an inactive caged precursor [17] at one flank of the protoplast by a localised pulse of short-wavelength light, and we followed the temporal changes of cell geometry at the illuminated versus the opposite non-illuminated flank of the protoplast.

## 2. Material and methods

### 2.1. Cell lines

Suspension cell cultures of salt tolerant *V. rupestris* and salt sensitive *V. riparia* [16] were cultivated in liquid medium containing 4.3 g·l<sup>-1</sup> Murashige and Skoog salts (Duchefa, Haarlem, The Netherlands), 30 g·l<sup>-1</sup> sucrose, 200 mg·l<sup>-1</sup> KH<sub>2</sub>PO<sub>4</sub>, 100 mg·l<sup>-1</sup> inositol, 1 mg·l<sup>-1</sup> thiamine, and 0.2 mg·l<sup>-1</sup> 2,4-dichlorophenoxyacetic acid (2,4-D), pH 5.8. Cells were subcultured weekly by inoculating 8–10 ml of stationary cells into 30 ml of fresh medium in 100 ml Erlenmeyer flasks. A tobacco BY-2 line expressing the actin-binding domain 2 of plant fimbrin in fusion with GFP under control of the constitutive CaMV-35S promoter was cultivated in the same media supplemented with hygromycin (30 mg·l<sup>-1</sup>) as described in [12]. This cell line was used as an actin marker line for *in vivo* observation of actin filaments. A second tobacco BY-2

cell line stably expressing Arabidopsis  $\beta$ -tubulin TuB6 fused to GFP [18] was used to follow microtubules *in vivo*. This cell line was cultivated in the same media supplemented with kanamycin (50 mg·l<sup>-1</sup>). The cell suspensions were incubated on an orbital shaker (KS250 basic, IKA Labortechnik, Staufen, Germany) at 25 °C in the dark with 150 rpm.

### 2.2. Visualisation of microtubules and actin microfilaments via immunofluorescence

Microtubules and actin microfilaments were visualised in suspension cells of *Vitis* as described by Qiao *et al.* [19]. Cells were observed under a confocal laser scanning microscope (TCS SP1; Leica, Germany) using a dual-wavelength (ArKr laser lines 488 and 564 nm) configuration, or under a AxioImager Z1 microscope (Zeiss, Göttingen, Germany) equipped with an ApoTome microscope slider for optical sectioning, and a cooled digital CCD camera (AxioCam MRm).

### 2.3. Generation of protoplasts

Protoplasts of *Vitis* were obtained by digesting suspension culture cells at specific time points after inoculation (day 7 to 9) with 1% w/v cellulase and 0.3% w/v macerozyme in slightly hypertonic medium (0.45 M mannitol) for 3–4 h in the dark at 25 °C on an orbital shaker at 100 rpm. For tobacco cells, 3-day-old cell culture was digested with 1% w/v cellulase and 0.1% w/v pectolyase in slightly hypertonic medium (0.45 M mannitol) for about 2 h under the same condition. Progression of digestion was followed till the most majority of the cells displayed a perfectly spherical shape. The liberated protoplasts were filtered with a nylon mesh of 70  $\mu$ m pore width and washed twice in slightly hypotonic medium (0.3 M mannitol). For the washing steps, protoplasts were collected by centrifugation at 300 rpm for 15 min. After the second washing step, the protoplasts were resuspended in a minimal amount of 0.3 M mannitol supplemented with 10% (v/v) of enzyme solution (1% w/v cellulase and 0.3% w/v macerozyme in 0.3 M mannitol) to suppress regeneration of new cell walls.

### 2.4. Pharmacological treatments

#### 2.4.1. Cell membrane agents

Benzyl alcohol (BA) is an amphiphilic molecule, which has been used often to investigate cellular responses to membrane fluidity. Benzyl alcohol can be used as a membrane “fluidizer” that affects lipid bilayer structures [20]. In contrast, dimethylsulfoxide (DMSO), a polar aprotic solvent, is a well-documented membrane rigidifier [21]. Aliquots of protoplast were treated with various concentrations of BA and DMSO for 30 min prior to the measurement.

#### 2.4.2. Elicitor treatments

Harpin is a protein from the phytopathogenic bacterium *Erwinia amylovora* and can induce so called effector-triggered immune responses [22]. A prominent feature of this type of immunity is the induction of rapid actin bundling [23].

Aliquots of protoplast were treated with 3 mg/mL Harpin (Messenger, EDEN Bioscience Corporation, Washington, USA; 3% of active ingredient Harpin protein, dissolved in MS liquid medium to a concentration of 300 mg/mL) for 30 min and then used for further analysis.

#### 2.4.3. Cytoskeletal drugs

Latrunculin B binds actin monomers near the nucleotide binding cleft with 1:1 stoichiometry and prevents actin from polymerizing, resulting in progressive elimination of the actin filaments depending on their innate turnover. Phalloidin binds specifically at the interface between F-actin subunits, locking adjacent subunits together, which prevents the depolymerisation of actin filaments. Aliquots of protoplast were treated with either 1  $\mu$ M Phalloidin (Sigma-Aldrich, Steinheim,

Germany) or Latrunculin B (Sigma-Aldrich) for 30 min and then used for experiments.

Taxol stabilizes the microtubule polymer against disassembly. Oryzalin sequesters the dimer of plant tubulin at the plus end, whereas depolymerisation at the minus ends proceeds resulting in progressive elimination of microtubules depending on their innate turnover. Aliquots of protoplast were treated with either 10  $\mu$ M of Taxol (Sigma-Aldrich) or Oryzalin (Sigma-Aldrich) for 30 min and then used in the following experiments.

All cytoskeletal drugs are not readily water soluble and have thus to be dissolved in DMSO as stock solutions and stored at 4 °C. For this reason, a solvent control with DMSO was included in the experiments to probe for potential effects of the solvent.

### 2.5. Determination of expansion velocity

To observe protoplast expansion, 5  $\mu$ l of protoplast suspension was mixed with 45  $\mu$ l of bidistilled water, and 20  $\mu$ l of the mixture were transferred into a hemocytometer (Fuchs-Rosenthal), and observed by differential interference contrast microscopy (Axioskop FS 2, Zeiss, Jena, Germany). The time of mixing was defined as starting time  $t = 0$ , images were recorded from 1 min after mixing at intervals of 30 s over the following 3 min. Protoplast diameters were determined using the AxioVision Rel. 4.8 software (Zeiss, Jena, Germany).

Osmolality of the solutions ( $c_o$ ) administered to the protoplasts was measured by a vapour pressure osmometer (Vapro 5520; Wescor Inc.). The readout values were converted to osmotic pressure and then used for calculating hydraulic conductivity  $L_p$  as described in [24].

Protoplast expansion velocity was calculated based on hydraulic conductivity  $L_p$  [24]:

$$L_p = (dV/dt)/(-\Delta\Pi) \approx [(V_{90s} - V_{60s})/30s]/[S(Om_s - Om_o)]$$

with  $V$ : protoplast volume;  $S$ : protoplast surface area;  $\Pi$ : osmotic pressure;  $Om_o - Om_i$ : osmotic gradient (outside–inside).

### 2.6. Analysis of membrane turnover by quantifying intensity of the FM4-64 tracer

Protoplasts of BY-2 cells were prepared as described above. They were then subjected either to hypoosmotic stress (final concentration of 0.15 M mannitol), or to hyperosmotic stress (final concentration of 0.5 M mannitol) in the presence of low concentrations (5  $\mu$ M) of the membrane tracer FM4-64 (Molecular Probes/Invitrogen, Carlsbad, CA, USA). Time-lapse series were recorded at intervals of 10 s, and average fluorescent intensities from at least 20 protoplasts were determined for each time point using the software Image J [25]. Relative fluorescent intensity compared to that of the first image was plotted over time.

## 3. Theory

### 3.1. Osmotic water permeability

By definition, the hydraulic permeability of a membrane,  $L_p$ , is the ratio of the area specific trans-membrane volume flux  $J_v$  to the difference in water potential  $\Delta\Psi$  across the membrane:

$$J_v = -L_p \Delta\Psi_w$$

In the current work,  $J_v$  is approximated by  $\Delta V/S\Delta t$ , where  $S$  is membrane area,  $V$  volume and  $t$  time. Because the turgor pressure (trans-membrane hydrostatic pressure) is negligible, here  $\Delta\Psi$  is well approximated by  $-\Delta\Pi$ . Therefore,

$$L_p \approx \frac{\Delta V/\Delta t}{S\Delta\Pi}$$

$\Delta\Pi = Osm_o - Osm_i$ : osmotic gradient (outside–inside). In case of a simple membrane,  $L_p$  would monitor the permeability of the membrane. However, in case of submembraneous membrane stores that are structured by the cytoskeleton and integrated into the expanding surface of the cell during swelling,  $L_p$  would not merely depend on membrane permeability, but on the dynamics of this integrative membrane–cytoskeleton network. Changes of permeability depend on the activity of aquaporins that are also present in the plasma membrane of plant cells and can be partially activated also independently of gene expression by phosphorylation [13]. Although the activity of aquaporins responds to osmotic fluctuations, significant aquaporin phosphorylation is not observed earlier than 15 min after the osmotic challenge [26], and thus is of minor impact during the time frame of the experiments reported here. Therefore, under the conditions of our assays,  $L_p$  depends not only on the flow of membrane material between submembraneous membrane stores and the cell surface, but also reports on mechanic constraints implied by the cytoskeleton.

### 3.2. Cytoskeleton and membrane structure

In our previous work, we have shown that a submembraneous population of actin contributes to the integrity of plant membranes challenged by pulsed electrical fields, and that actin together with microtubules form radial arrays in immediate vicinity of the plasma membrane close enough (<50 nm) to be imaged by total internal reflection fluorescence (TIRF) microscopy [12], which led us to a model, where the plasma membrane entertains a dynamic equilibrium with a submembraneous tubulovesicular reservoir of membrane material maintained and mobilised by the cytoskeleton. In the context of this model, swelling would involve rapid signalling of osmotic strains on the membrane upon the cytoskeleton that would respond by rapid disassembly and/or reorganisation. The transduction of mechanic load on biomembranes into biochemical events is conventionally explained by two alternative mechanisms: Stretching of membrane-associated biomolecules will change their conformation and create new interaction sites with other biomolecules (for reviews see [27,28]. Alternatively, mechanosensitive channels read out directly a detectable response to forces from the lipid bilayer (for review see [1]). Such mechanosensitive calcium channels have been reported for plant cells (for a recent review see [29]), are important for the activation of plant defence, and can be inhibited by gadolinium ions [30]. However, activation of cytoskeletal reorganisation by stretching of membrane-associated biomolecules might be more relevant: the formation of tubulin aggregations (so called macro-tubules) induced by hyperosmotic stress can be blocked by *n*-butanol, a specific activator of membrane bound D-type phospholipases (PLD), which diverts the PLD function towards phosphatidylbutanol (PtdBut) instead of forming phosphatidic acid (PA) and the latter is more relevant for signalling [31]. In fact, T-DNA insertion into the PLD gene affects the response of *Arabidopsis thaliana* to drought stress [32]. Recently, an isoform of phospholipase Ds, NtPLD $\alpha$ 1 and its cleavage product PA were discovered to be important regulators in the membrane–actin interface of pollen tubes [33]. Interestingly, p90, a specific PLD isoform from tobacco, had been identified as membrane linker of plant microtubules [34] suggesting phospholipases of the D type as signalling hub controlling the interaction between plasma membrane and cytoskeleton [35]. Altogether, it is inferred that membrane deformations, for instance imposed by osmotic challenge, might render membrane lipids more accessible to phospholipase D, providing a mechanism to transduce mechanic load on the membrane into changes of cytoskeletal dynamics. However, signalling could also act in a retrograde manner, where mechanosensing by the cytoskeleton would be transduced to phospholipase D and thus modulate signalling. In fact, a growing microtubule is subject to considerable internal tension, caused by a conformational change of tubulin dimers shortly after integration [36]. This tension is balanced by a complex of so called + TIP proteins that constrain the outward bending of

the microtubule protofilaments and anchor the microtubule plus end with actin and other organelles including the plasma membrane. In fact, in *A. thaliana*, salt stress was shown to detach a plant specific member of the (+)-end-tracking proteins (+TIPs) called SPIRAL1 from this complex leading to increased microtubule catastrophe events [37]. This mechanism lead to the hypothesis that a similar regulation process might mobilise the submembraneous reservoirs for integration into the membrane during swelling within a much shorter time scale.

Phospholipase D can be activated by *n*-butanol, whereby *n*-butanol simultaneously acts as alternative transphosphatidyl substrate and results in the production of PtdBut instead of PA, which is not active

in the context of signalling [38]. In contrast, *sec*-butanol can activate phospholipase D, but is not accepting phosphatidic acid. Since phosphatidic acid is widely considered as the relevant signal (for a recent review see [39]), *n*-butanol, through activation of PLD, will block signalling, whereas *sec*-butanol should not. In fact, *n*-butanol, but not *sec*-butanol, can cause depolymerisation of cortical microtubules in *A. thaliana* [40] consistent with trans-phosphatidyl being required for this effect. This was explained by a model, where the transfer of the phosphatidyl moiety to phospholipase would cleave the membrane-interaction of microtubules leading to their destabilisation [41]. However, this model is challenged by reports that *n*-butanol can disrupt microtubules in

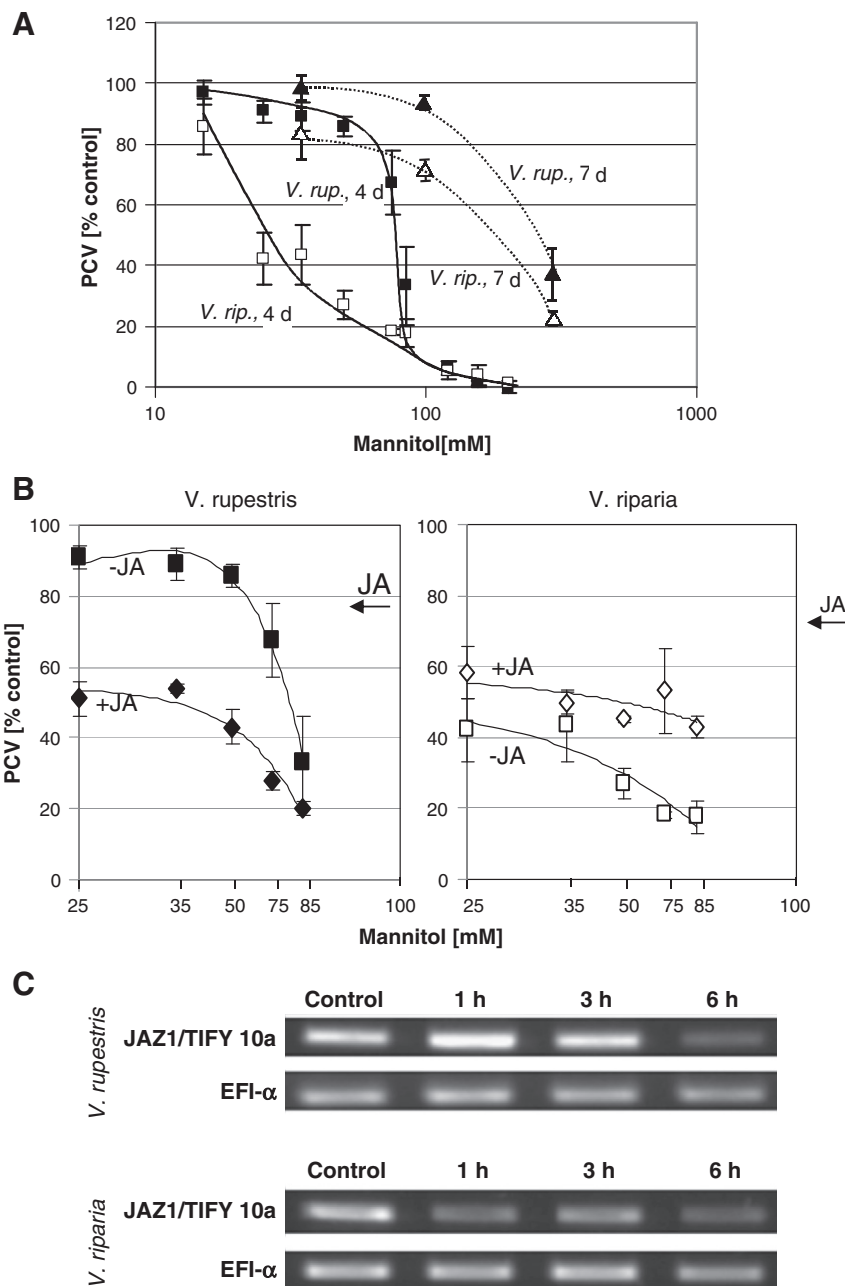


**Fig. 1.** Osmotic adaptation in *V. rupestris* and *V. riparia*. **A.** Dose–response of suspension cell culture growth (measured as packed cell volume, PCV) over the concentration of mannitol in the medium in *V. rupestris* (closed symbols) versus *V. riparia* (open symbols) assessed at day 4 (squares, solid curves), and, after adaptation, at day 7 (triangles, dotted curves). PCV was determined relative to controls cultivated in the absence of mannitol. Data points represent mean values and standard errors from three independent experimental series. **B.** Stimulation of osmotic adaptation by 30  $\mu$ M of exogenous jasmonic acid manifest as increase in relative PCV at day 4 in *V. rupestris* (left) versus *V. riparia* (right). Arrows indicate the values obtained for 30  $\mu$ M jasmonic acid in the absence of mannitol. Data points represent mean values and standard errors from three independent experimental series. **C.** Abundance of transcripts for JAZ1/TIFY 10 $\alpha$  as marker for osmotic adaptation in *V. rupestris* (top) versus *V. riparia* (bottom). Representative experiment is shown and a quantification of the transcript levels from three independent experimental series is given in Suppl. Fig. S1.

*vitro*, and that microtubules remain attached to the plasma membrane of tobacco protoplasts after treatment with *n*-butanol [42]. Moreover, in stramenopile cells, also *sec*-butanol can induce microtubule depolymerisation, suggesting that an alternative pathway independent of PA can convey the signal from phospholipase D activation to cytoskeletal downstream targets [43]. Since, *n*-butanol is consumed during activation of phospholipase D, whereas *sec*-butanol is not, *sec*-butanol causes a more stable activation of phospholipase D [38] and should be more efficient in phosphatidic-acid independent signalling.

### 3.3. Membrane turnover during cell volume control

Plant cells can undergo significant and repetitive changes in cell volume within minutes which consequently requires alteration in cell surface area over short time periods. This phenomenon is impressively illustrated by the rapid opening and closure of stomata by reversible expansion of guard cells. The limited stretching ability of plasma membrane (only up to 2%) [3] is not able to meet these challenges to the alteration of cell surface (up to 40%) [44]. Therefore, these challenges must be met by a tight and alert regulation of plasma-membrane turnover. Two mechanisms are conceivable to achieve these alterations of membrane surface: either, the membrane can be folded or unfolded, or membrane material from submembrane stores is rapidly removed or inserted. Evidence for both mechanisms has been reported [4,45,46]. However, it is unclear, how plant cells can sustain the high activity of endocytosis against the turgor pressure, and how the large numbers of vesicles are sorted and retrieved/integrated from/into the membrane [47]. Moreover, the quantification of membrane turnover is far from trivial [45], due to the resolution limit of light microscopy, only vesicles with diameter over 300 nm can be detected, for instance upon staining with fluorescent membrane markers. The detection limit for membrane integration events using patch-clamp can reach 60 nm. However, vesicles as small as 20 nm have been observed by electron microscopy during stomatal closure in *Vicia faba* L. [45].

For these reasons, it is not possible to observe the membrane flow directly. To circumvent these constraints, we use in the current work the property of the styryl dye FM4-64 that acquires fluorescence upon integration into the plasma membranes. Under control conditions, for a low concentration of the dye, the fluorescent intensity should, upon mixing, remain constant and then slowly decrease due to bleaching of the fluorophore. When new membrane material is integrated into the stained plasma membrane, this will first expose additional binding sites for the FM4-64 molecules diffusing freely in the medium surrounding the protoplasts leading to a transient increase of fluorescence intensity. However, for a low background concentration of the dye, this increase will be limited. When now additional membrane material is integrated, the average fluorescence intensity will decrease faster than in the control, because loss of intensity from bleaching will add up with the dilution of fluorescence by the integration of additional (unlabelled). When membrane material is retracted from plasma membrane via endocytosis or infolding this will result in contraction of fluorescent material and thus an increase of average fluorescence overlaid with the bleaching. As a result, compared to the control, average fluorescence intensity will decrease more slowly. Thus, the dynamic changes at the plasma membrane can be monitored by recording time series and quantify relative changes in the average pixel fluorescent intensity using quantitative image analysis.

Based on these considerations, several predictions for  $L_p$  can be derived which can be tested experimentally: (i)  $L_p$  should be altered by compounds targeted to actin, (ii)  $L_p$  should also be altered by compounds targeted to microtubules, (iii)  $L_p$  should neither significantly respond to gadolinium nor to quenching of extracellular calcium nor to fluidisation of the membrane, (iv) local dissociation of actin cables should cause local mobilisation of membrane stores and thus to a local deformation (bulging) of the protoplast, (v) treatment with BA and DMSO could help to judge if and how membrane fluidity affects  $L_p$ , (vi) treatment

with *n*-butanol versus *sec*-butanol should allow to discriminate, whether phospholipase D signalling acts through the phosphatidic acid dependent or independent pathway if their role as membrane fluidiser has been ruled out depending on the outcome of DMSO and BA treatments, (vii) fluorescent intensity of FM4-64 should undergo increase or decrease when subjected to hypo- or hyper-osmotic stress if membrane turnover respond to osmotic pressure by membrane integration/unfolding or retrieval/folding.

## 4. Results

### 4.1. Adaptation to hyperosmotic stress is more pronounced in *V. rupestris*

The two cell lines had been shown earlier to differ in salt tolerance [16]. To test whether the tolerance to salt results from differences in  $\text{Cl}^-$  or  $\text{Na}^+$  toxicity or from differences in osmotic adaptation, we recorded dose–response curves of culture growth (measured as relative packed cell volume, PCV) over mannitol as osmolyte (Fig. 1A). In both cell lines, growth was inhibited completely after 4 days when 100 mM of mannitol was added to the cultivation medium. However, the thresholds of growth inhibition differed strongly – in *V. riparia*, already 25 mM of mannitol blocked growth by more than 50%, whereas in *V. rupestris* 85 mM of mannitol were required to reach the same level of inhibition. When we measured the PCV at day 7, growth was found to be recovered even for high concentrations of mannitol treatment in both cell lines, indicating progressive osmotic adaptation. Even at this stage, *V. riparia* was clearly more affected by mannitol as compared to the more tolerant *V. rupestris*. Similar to salt tolerance, osmotic tolerance can be rescued by exogenous jasmonate in *V. riparia* although not completely. In *V. rupestris*, where innate osmotolerance is already high, exogenous jasmonate cannot elevate osmotolerance further, but acts inhibitory, indicating that the overall levels of jasmonate are super optimal. We further measured the abundance of transcripts for JAZ1/TIFY 10a as marker for the activity of the jasmonate pathway (recording the activity of stress signalling) and observed a clear transient induction in *V. rupestris* with a peak at 1 h after the onset of hyperosmotic stress, whereas in *V. riparia* no induction was detectable (Fig. 1C, Suppl. Fig. 1). Thus, the differences in osmotolerance between the two grapevine cell lines are located upstream of jasmonate signalling.

### 4.2. The cytoskeleton of *V. rupestris* is more responsive to hyperosmotic stress

To obtain insight into the role of the cytoskeleton in the response to osmotic stress, microtubules in the suspension culture of both *Vitis* cell lines were visualised by immunofluorescence 30 min after addition of mannitol (Fig. 2A). Whereas in control cells microtubules were arranged in fine parallel bundles around the cell periphery for both *V. rupestris* and *V. riparia*, hyperosmotic treatment produced disoriented, partially disintegrated, and often rod-shaped tubulin bundles, similar to the macro-tubules described for hyperosmotically challenged *Triticum turgidum* cells [10]. This microtubular reorganisation was more pronounced in *V. riparia* and already observed for 50 mM mannitol, whereas in *V. rupestris* even at 100 mM mannitol microtubules were bundled, but still maintained most of their integrity. Actin filaments were visualised by fluorescent phalloidin (Fig. 2B) in cells that had been fixed at the same time point (30 min) after addition of mannitol. In control cells, microfilaments showed the typical organisation characteristic for vacuolated plant cells: a radial network converging on the nucleus is interconnected with a finer meshwork in the cell periphery. The cortical actin strands were thicker in *V. rupestris* as compared to *V. riparia*. Upon hyperosmotic treatment the radial network contracted towards the nucleus, whereas the cortical meshwork faded out. However, in plasmolytic cells, the shrinking plasma membrane (white arrows) was lined with dense bundles of actin. The overall integrity of the actin

cytoskeleton persisted somewhat better in *V. rupestris* as compared to *V. riparia*.

#### 4.3. Plasma membrane turnover responded to osmotic stress monitored by FM4-64 intensity

To get insight into temporal changes of membrane turnover, we quantified relative changes of average fluorescence intensity after FM4-64 during hypo- and hyper-osmotic stress (see supplementary data Fig\_Suppl\_2). Under isotonic control conditions, values were first constant for the first 10 s of observation (70 s after addition of the dye) suggesting that the binding of the dye was equilibrated at this time. Then, average intensity began to decrease slowly, which is expected from the bleaching in the course of fluorescence excitation. For hypotonic conditions, average fluorescence intensity transiently increased (consistent with the exposure of additional binding sites for the dye), but only slightly (by about 10%) indicating that the concentration of free dye was limiting, subsequently, the values decreased, but more rapidly than in the control, as to be expected from active integration of unlabelled membrane material diluting the stained plasma membrane. For protoplasts subjected to hyperosmotic pressure, the decrease of average intensity was much slower than in the control, consistent with the prediction that membrane material stained by the dye was contracted. Pretreatment of the protoplasts with *n*- or *sec*-butanol did not alter the fading pattern of fluorescent intensity compared to the control when exposed to hypotonic solution.

#### 4.4. Osmotic water permeability depends on the cytoskeleton

To obtain quantitative data on the role of the cytoskeleton for osmoregulation, we determined  $L_p$  after treatment with cytoskeletal agents (Fig. 3A). Values for  $L_p$  were derived from time series, where protoplasts were transferred into a hypoosmotic medium (distilled water) at  $t = 0$  and then recorded from  $t = 60$  s at intervals of 30 s

(Fig. 3B). Since the protoplasts form ideal spheres, the volume could be easily deduced from the cross-sections. To validate this approach to estimate  $L_p$ , temporal changes of  $L_p$  were determined for 73 time series and found to be <5% (Fig. 3C). Thus, protoplast swelling is approximately linear such that the obtained value of  $L_p$  is mostly independent of the time point used for its determination within the range tested. Using the same series we probed for a potential dependency of  $L_p$  and the surface calculated for the individual protoplasts (Fig. 3D), but we did not detect any significant correlation. Thus,  $L_p$  turned out to be a robust parameter which depends neither on the time point of measurement nor on the individual differences in protoplast size.

In the next step, we determined  $L_p$  after pharmacological manipulation of specific cellular targets. When microtubules were eliminated by Oryzalin (Fig. 4A),  $L_p$  increased by 30% in both cell lines, whereas stabilisation of microtubules by Taxol decreased  $L_p$  by around 20% (more pronounced in *V. rupestris* as compared to *V. riparia*). When actin filaments were eliminated by Latrunculin B,  $L_p$  increased by 20–25% in both cell lines, treatment with Phalloidin did not produce significant changes in  $L_p$ . Since the response of *V. rupestris* and *V. riparia* followed the same pattern, just at different amplitude, we focussed the subsequent experiments on *V. rupestris*. To calibrate the amplitude of the changes in  $L_p$  after treatment with cytoskeletal drugs, we permeabilised the membrane by DMSO and obtained an increase of  $L_p$  at 35% for 1% v/v DMSO (Fig. 4B), which could not be raised further by higher concentrations (2% v/v). This means that the response obtained with Oryzalin almost sustained the level for unimpaired water influx, and Latrunculin B produced more than half of this level. We then increased membrane fluidity by benzyl alcohol which increases the spacing between phospholipid chains, but did not observe any significant effect on  $L_p$  even for 8 mM benzyl alcohol, a concentration that can completely compensate cold induced membrane rigidification in *Brassica napus* [48]. Likewise, neither chelation of extracellular calcium by EGTA nor blocking calcium influx by gadolinium ions had any significant effect on  $L_p$ . However, treatment with the bacterial effector Harpin that causes

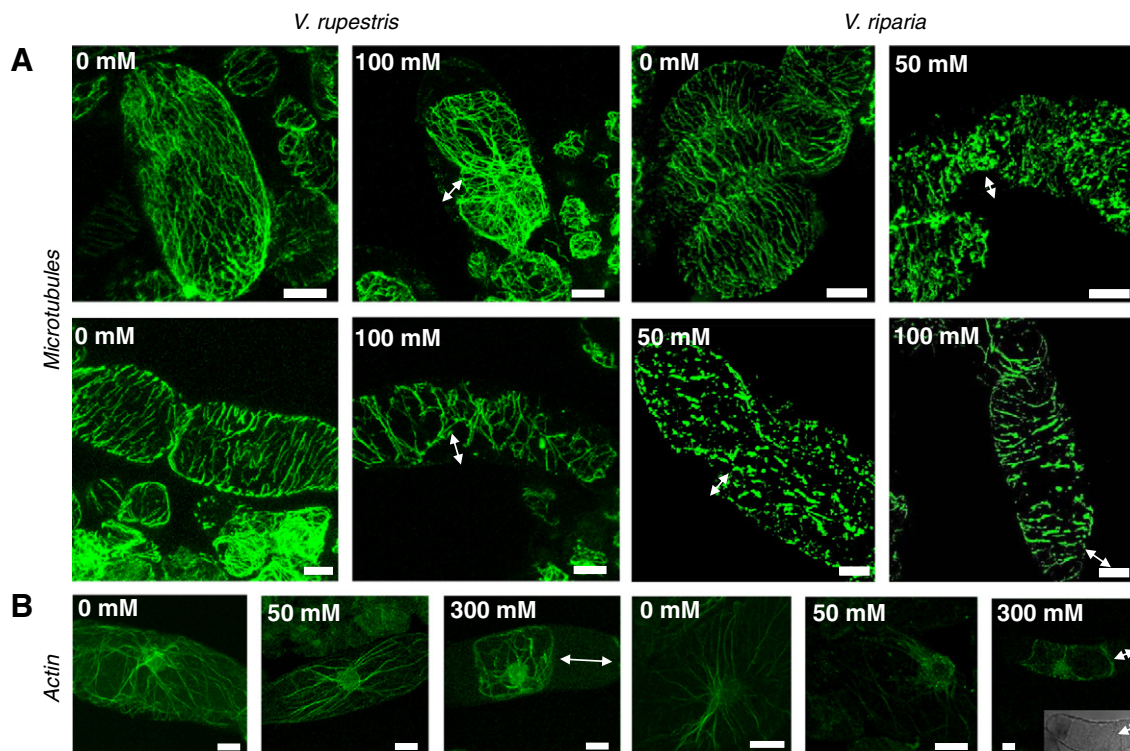
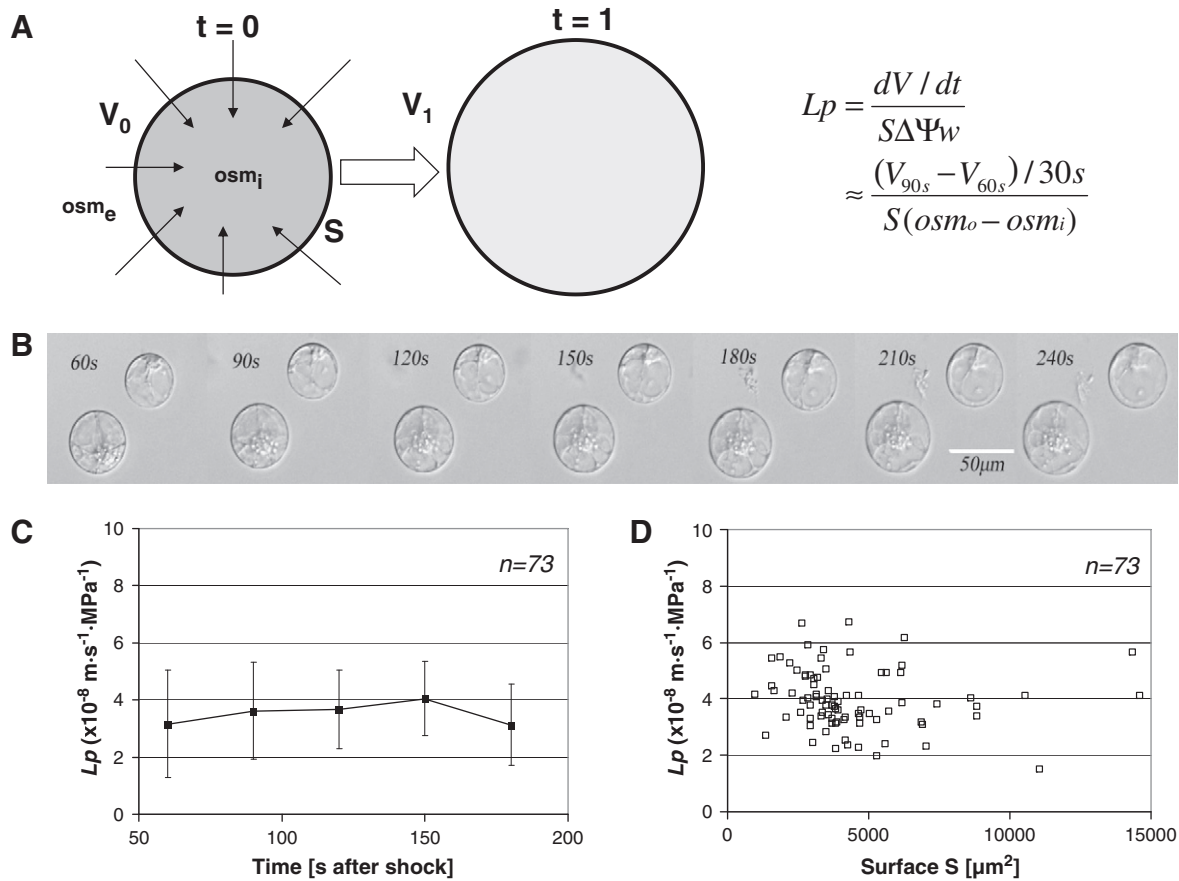


Fig. 2. Response of microtubules (A) and actin filaments (B) to hyperosmotic stress in *V. rupestris* and *V. riparia*. Cells were treated with mannitol for 30 min and then fixed directly for immunofluorescent visualisation of microtubules (A) or phalloidin staining of actin filaments (B), respectively. Double-headed arrows indicate plasmolysis. Size bar 20  $\mu$ m.



**Fig. 3.** Determination of osmotic water permeability (hydraulic conductivity)  $L_p$ . **A.** Set-up of experiment. At time 0, a protoplast is transferred into distilled water ( $osm_e = 0$ ), and the increase in volume over the time was determined from photographic images of the protoplast based on the spherical geometry. **B.** Representative time series for two protoplasts of *V. rupestris* transferred at time 0 s into distilled water. **C.** Dependence of temporal changes of  $L_p$  on the time after transfer into distilled water calculated as mean and standard error from 73 individual time courses. Temporal changes of  $L_p$  remain <5%. **D.** Dependence of mean values  $L_p$  on the initial surface  $S$  based on 73 individual time courses. There is no correlation between initial surface  $S$  and time.

massive bundling of actin in *V. rupestris* [19] reduced  $L_p$  by about 10%. To test a possible role of phospholipase D [31], we tested the influence of the phospholipase D activators *n*-butanol and *sec*-butanol [38]. We observed that both compounds increased  $L_p$  (Fig. 4B) (compare Fig. 4A and B).

At the same time, protoplasts generated from the tobacco BY-2 actin marker line GF-11 and the microtubule marker line  $\beta$ -Tub6 were treated with cytoskeletal drugs at the present of either hypo- or hyper-osmotic pressure to follow the cytoskeletal response to osmotic stress and cytoskeletal drugs *in vivo*. In control protoplasts (see supplementary data Fig\_Suppl.\_3A), actin showed the characteristic organisation, with a fine network underneath the plasma membrane, and a radial array of actin cables tethering the nucleus (termed as perinuclear actin basket). In hypotonic solution, actin filaments were redistributed towards the membrane, whereas the perinuclear actin basket appeared depleted. In contrast, transfer into hypertonic solution partitioned actin towards the perinuclear actin basket, whereas the membrane associated actin vanished (see supplementary data Fig\_Suppl.\_3A). Treatment with Latrunculin B produced a general depletion of actin, whereby the membrane associated actin arrays were affected stronger than the perinuclear network consistent with a higher dynamics of the membrane-associated actin. Most prominently, the partitioning of actin towards the membrane under hypoosmotic conditions was suppressed by Latrunculin B. Treatment with phalloidin, in contrast, caused a contraction of actin towards the nucleus. Microtubules form radial bundles emanating from the nucleus. These bundles were eliminated by Oryzalin treatment and widened by Taxol treatment (see supplementary data Fig\_Suppl.\_3B). Hypoosmotic shock caused generally a depletion of the microtubular cytoskeleton. Oryzalin promoted, Taxol reduced this depletion. For hyperosmotic

shock, microtubules contracted towards the nucleus and appeared wider. This contraction was less pronounced in presence of Oryzalin, and promoted by Taxol. Generally, during hyperosmotic shock, the protoplasts deviated from a spherical shape, most pronounced, when the microtubules were eliminated. These results showed that the cytoskeleton in protoplasts reorganised in response to hypo- and hyper-osmotic stress, and that cytoskeletal drugs modulate these responses.

#### 4.5. Local dissociation of actin cables causes local bulging of the protoplast

The increases in  $L_p$  might be caused by increased mobilisation of submembraneous reservoirs of membrane material. However, direct changes of aquaporin activity cannot be ruled out *a priori*. To discriminate between these two possibilities, we used optochemical engineering of actin organisation. Actin bundles can be dissociated into fine strands by the plant hormone indolyl-3-acetic acid. Inactive derivatives, where the active hormone is blocked by a photoactivable 'cage' can be used to release the active hormone by a light beam at cellular resolution and using this approach we were able to dissociate actin bundles at sub-cellular resolution [17]. We used this approach under slightly hypotonic conditions to release actin rigidity at one flank of a protoplast by a beam of activating light, whereas it would remain unaltered in the opposite, non-illuminated, flank of the protoplast. If actin would limit  $L_p$  by a constraint on aquaporin activity, the illumination should increase membrane porosity, such that the cell would swell slightly. Due to the isotropic action of turgor pressure, the swelling would spread all over the cell and hardly be detectable. If actin would limit  $L_p$  by a constraint on the mobilisation of submembraneous membrane material, the

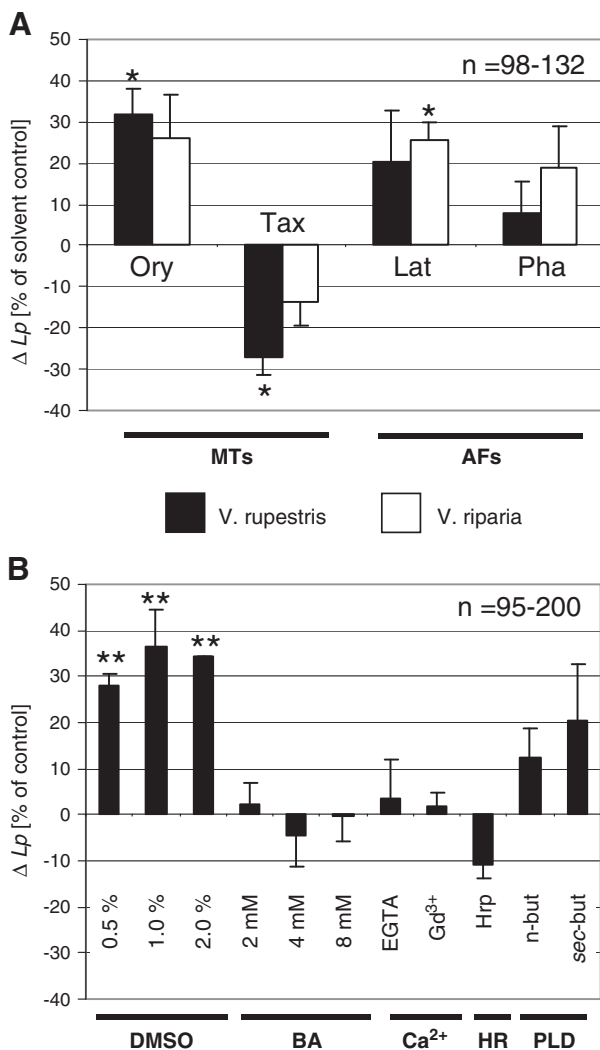


**Fig. 4.** Effect of pharmacological manipulation of cellular targets on  $L_p$ . **A.** Effect of drugs acting on microtubules (MTs) or actin filaments (AFs). Relative change of  $L_p$  plotted for *V. rupestris* (black bars) and *V. riparia* (white bars) after pretreatment with 10  $\mu$ M Oryzalin (Ory), 10  $\mu$ M Taxol (Tax), 1  $\mu$ M Latrunculin B (Lat), and 1  $\mu$ M Phalloidin (Pha), respectively, as compared to the solvent control. **B.** Effect of membrane permeabilisation (DMSO), membrane fluidisation (BA), calcium depletion (EGTA, 1 mM), block of calcium influx ( $Gd^{3+}$ , 80  $\mu$ M), induction of a hypersensitive reaction (Hrp, 9  $\mu$ g.ml<sup>-1</sup>), and activation of phospholipase D (PLD, 0.5% of *n*-butanol or *sec*-butanol) in *V. rupestris*. All pretreatments started 30 min prior to the hypoosmotic shock. Data show mean values and standard errors from 98 to 132 (A) and 95–200 (B) individual time courses collected from 3 to 5 independent experimental series. \* $P < 0.05$ , \*\* $P < 0.01$ , Student's *t* test.

illuminated flank should bulge by local extension of the cell surface. We tested these predictions in tobacco BY-2 protoplasts expressing the actin marker GFP fimbrin actin-binding domain 2 to be able to follow the response of actin filaments *in vivo*. We observed that actin cables had already initiated dissociation at 10 min after the light pulse. In parallel, the protoplast lost its initial circularity (see [supplementary data Fig\\_Suppl\\_4A](#)). To analyse this loss of circularity in more detail, the local asymmetry was plotted over the azimuth starting from the site of illumination (see [supplementary data Fig\\_Suppl\\_4B](#)). Asymmetry was defined as relative difference  $(r - r_0)/r_0$  at a given azimuth and  $r_0$  as mean distance between cell centre and cell membrane (see [supplementary data Fig\\_Suppl\\_4C](#)). In case of a perfect circle, this plot would yield a straight horizontal line. Using this parameter, already from 10 min a clear break of symmetry became detectable (see [supplementary data Fig\\_Suppl\\_4B](#)). When time courses of asymmetry were plotted for fixed azimuth angles (see [supplementary data Fig\\_Suppl\\_4C](#)), it became evident that, in the equator between

illuminated and shaded flank, symmetry was mostly maintained, whereas in the illuminated flank ( $=0^\circ$ ) asymmetry had already significantly increased at 10 min after the light pulse reaching a saturation value of  $\sim +30\%$  at 30 min after the pulse. In contrast, the shaded flank ( $=180^\circ$ ) attained negative values reaching a saturation of  $\sim -20\%$  at 30 min after the pulse. This means that the protoplast bulges out in the illuminated flank and flattens in the shaded flank. The bulging in the lighted flank is more pronounced than the flattening in the shaded flank.

## Discussion

Different mechanisms have been proposed for the role of the cytoskeleton in volume control [49,13]: (1) the cortical cytoskeleton might regulate (osmosensory) ion-channel activity and thus limit water uptake, or it might regulate (downstream) mass transport across the membrane. (2) Transvacuolar bundles of actin might impede protoplast swelling by mechanic tethering (for microtubules that do not harbour tensile resistance, but only compressive resistance, such a mechanism would not work). (3) The dynamic cortical cytoskeleton might adhere to the plasma membrane, and control the mobilisation of material into the expanding membrane. In the following, we will discuss our experimental results in the conceptual framework of these three mechanisms.

Protoplast swelling is based on osmotic water influx and requires the incorporation of additional material into the expanding membrane [46]. The initial stimulus is the osmotically generated force upon the membrane resulting from water influx, which might be sensed by mechanosensitive ion channels [1]. In plants, the molecular base of mechanosensitive channel activities remains to be elucidated, but is thought to involve calcium influx [50]. However, neither  $Gd^{3+}$  ions, inhibitors of mechanosensitive calcium channels, nor the calcium chelator EGTA had any significant effect on the  $L_p$  values (Fig. 4B), consistent with previous work on guard cell protoplasts, where changes of plasma membrane surface (monitored via membrane capacitance) in response to osmotic stimuli were also found to be independent of calcium [51]. The cytoskeletal regulation of  $L_p$  is therefore unlikely to be caused by cytoskeletal gating of the sensory calcium channels. Since  $L_p$  records a combination of net water influx and plasma-membrane incorporation, the cytoskeletal effect on swelling might be caused by a modulation of mass flux, for instance of net water influx. We therefore manipulated the organisation of actin by optochemical engineering in isotonic conditions and could by this treatment induce a symmetry break with a local bulging at the illuminated side (see [supplementary data Fig\\_Suppl\\_4A](#)). Since pressure is non-directional, the amplitude of this bulging is limited, but clearly the effect on actin is not global, but locally confined (consistent with published evidence on walled cells [17]). Under these conditions, net influx of water should be zero. Therefore, we conclude that the cytoskeletal effect on volume increase is independent of ion channel and water channel activities.

Intensive expansion ability of plasma membranes is confined to  $\sim 2\%$  [52] and occurred only during the first few seconds after being transferred into hypoosmotic medium. We tested therefore, whether  $L_p$  can be modulated by altering the extensive properties of the membrane. Treatment with benzyl alcohol which increases the fluidity of lipid bilayers [48] did not cause any significant change of  $L_p$  (Fig. 4B). Since the membrane fluidizer BA did not alter  $L_p$ , a potential activity of both butanols used in our experiments as membrane fluidizers is obviously not helpful to explain, why they promote  $L_p$ . This promotion is more probably linked with their enzymatic activities. In contrast, DMSO, which has been used as membrane stabiliser in a study on cold adaptation of plant cells [48], increased  $L_p$  values. However, DMSO is not only stabilising membranes, but also causes a permeabilisation, which in the context of our experiment increases the water permeability of the membrane [53]. It is therefore not surprising that we observed increased  $L_p$  values after treatment with DMSO. Thus, our data do not

support a model, where intensive changes of the membrane play any role for the observed swelling response.

Thus, the volume increase must be supported by incorporation of additional membrane material or unfolding of membrane invaginations. Direct tracking of endocytosis is limited by the small size of the vesicles that are smaller than the resolution limit for light microscopy. We therefore quantified relative changes in the intensity of the membrane dye FM4-64 to monitor membrane dynamics during hypo- and hypertonic stress. Our data indicated that new membrane material was inserted into the expanding plasma membrane during hypotonic stress, whereas membrane material contracted during hypertonic stress. The role of the cytoskeleton in this process might be twofold: either mere mechanic stabilisation of the membrane leading to a resisting tension. Alternatively, the cytoskeleton might control the mobilisation of membrane resources during swelling. In this functional context, the cytoskeleton might either convey the transport of membrane material to the membrane (stimulating function), or constrain the release of the material during the integration itself (impeding function). When osmotic tension exceeds the resistance tension, and if no more resources of membrane material can be mobilised, this would lead to protoplast lysis. The situation for microtubules seems to be straightforward. We observe that  $L_p$  values increase after treatment with the microtubule-eliminating agent Oryzalin, and decrease after stabilisation of microtubules by Taxol (Fig. 4A). Activation of phospholipase D by *n*-butanol increases  $L_p$ , as to be expected from microtubule detachment from the membrane (Fig. 4B). This activity seems to be independent of phosphatidic acid synthesis by phospholipase D, since *sec*-butanol is as effective as *n*-butanol. The *V. riparia* cell line that is more susceptible to hyperosmotic stress (Fig. 1), shows a reduced response of the osmoadaptive marker JAZ1/TIFY 10a (Fig. 1C, Suppl. Fig. 1), and a reduced osmotolerance of the cytoskeleton (Fig. 2). Consistently, this line was also somewhat less responsive to the microtubule drugs Oryzalin and Taxol with respect to  $L_p$  (Fig. 4A). Since the effect of both drugs depends on the innate turnover of microtubules, this indicates that microtubules are less dynamic in *V. riparia* as compared to *V. rupestris*, which is supported by previous findings of a higher degree of tyrosinylated  $\alpha$ -tubulin, a marker for cycling tubulin [19]. Microtubules might therefore simply impede membrane material from being inserted into the expanding membrane.

The role of actin seems to be more complex. Here, elimination of actin by Latrunculin B caused an increase of  $L_p$  values. However, a mild treatment with Phalloidin, a drug suppressing disassembly of F-actin does not cause a decrease, but an increase of  $L_p$  as well, which although not statistically significant, worth paying attention. This might be linked with differences in the cellular target sites of the two drugs seems to differ (Supp. Fig. 3A): Latrunculin B depleted membrane associated actin and suppressed the repartitioning of actin towards the membrane observed in hypoosmotic conditions. Phalloidin, however mainly targeted to the perinuclear actin cables. A stimulating role of actin stability is consistent with previous findings, where the same concentration of Phalloidin [11] or inducible expression of an actin-binding domain [12] stabilised the membrane against electric permeabilisation. In *V. riparia*,  $L_p$  values were more responsive to actin drugs as compared to *V. rupestris*, indicating a higher innate turnover of submembraneous actin in *V. riparia* over *V. rupestris*. These observations suggest a positive role of actin stability for swelling, which might involve actin-driven transport of membrane resources towards the insertion sites. It should be noted that these (positive) effects of actin stability are different from the (negatively acting) massive bundling of transvacuolar actin cables induced by hyperosmotic shock (Fig. 2B) or the Harpin elicitor [19]. These cables mechanically simply impair protoplast expansion independent of membrane integrity.

## 6. Conclusions

We dissected the role of actin filaments and microtubules for regulatory volume increases by monitoring apparent water permeability

values after pharmacological manipulation of different cellular targets. We can exclude a role of calcium channel activity or extensive changes of membrane extensibility for the swelling response. We conclude that a dynamic population of microtubules impedes the integration of membrane material into the expanding membrane. This microtubule population can be controlled by activation of phospholipase D independently of phosphatidic acid synthesis. In contrast, a dynamic population of actin acts as positive regulator of protoplast swelling. Bundling of transvacuolar actin cables by the Harpin elicitor can block expansion, probably by merely mechanic tethering. Actin dynamicity can be upregulated by the plant hormone auxin [54]. Using this phenomenon, we demonstrated that a localised protoplast expansion can be triggered even under isotonic conditions using optochemical engineering with caged auxin consistent with a model, where actin dynamicity supports the delivery of membrane resources into expanding membrane during hypotonic challenge.

Supplementary data to this article can be found online at <http://dx.doi.org/10.1016/j.bbame.2013.04.027>.

## Acknowledgements

This work was supported by fellowships of the China Scholarship Council (CSC) to Qiong Liu and Fei Qiao, a DAAD-GERL fellowship to Ahmed Ismail and a Visiting Scholarship of Karlsruhe House of Young Scientist (KHYS) to Fei Qiao. Sabine Purper (Karlsruhe Institute of Technology) is acknowledged for the excellent technical assistance during establishment of the cell cultures.

## References

- [1] C. Kung, A possible unifying principle for mechanosensation, *Nature* 436 (2005) 647–654.
- [2] J.H. Henson, Relationships between the actin cytoskeleton and cell volume regulation, *Microsc. Res. Techn.* 47 (1999) 155–162.
- [3] J. Wolfe, M.F. Dowgert, P.L. Steponkus, Mechanical study of the deformation and rupture of the plasma membranes of protoplasts during osmotic expansions, *J. Membr. Biol.* 93 (1986) 63–74.
- [4] U. Kubitschek, U. Homann, G. Thiel, Osmotically evoked shrinking of guard-cell protoplasts causes vesicular retrieval of plasma membrane into the cytoplasm, *Planta* 210 (2000) 423–431.
- [5] J.C. Shope, D.B. DeWald, K.A. Mott, Changes in surface area of intact guard cells are correlated with membrane internalization, *Plant Physiol.* 133 (2003) 1314–1321.
- [6] E. Zeiger, P.K. Hepler, Light and stomatal function: blue light stimulates swelling of guard cell protoplasts, *Science* 196 (1977) 887–889.
- [7] M. Koivusalo, A. Kappus, S. Grinstein, Sensors, transducers, and effectors that regulate cell size and shape, *J. Biol. Chem.* 284 (2009) 6595–6599.
- [8] E.A. Papakonstanti, E.A. Vardaki, C. Stournaras, Actin cytoskeleton: a signaling sensor in cell volume regulation, *Cell. Physiol. Biochem.* 10 (2000) 257–264.
- [9] G. Komis, P. Apostolakis, B. Galatis, Hyperosmotic-stress induced actin filament reorganization in leaf cells of *Chlorophytum comosum*, *J. Exp. Bot.* 53 (2002) 1699–1710.
- [10] G. Komis, P. Apostolakis, B. Galatis, Hyperosmotic stress induces formation of tubulin macro-tubules in root tips of *Triticum turgidum*: their probable involvement in protoplast volume control, *Plant Cell Physiol.* 43 (2002) 911–922.
- [11] T. Berghöfer, C. Eing, B. Flickinger, P. Hohenberger, L.H. Wegner, W. Frey, P. Nick, Nanosecond electric pulses trigger actin responses in plant cells, *Biochem. Biophys. Res. Commun.* 387 (2009) 590–595.
- [12] P. Hohenberger, C. Eing, R. Straessner, S. Durst, W. Frey, P. Nick, Plant actin controls membrane permeability, *BBA Biomembranes* 1808 (2011) 2304–2312.
- [13] C. Maurel, Aquaporins and water permeability of plant membranes, *Annu. Rev. Plant Physiol. Plant Mol. Biol.* 48 (1997) 399–429.
- [14] O.M. Nesin, O.N. Pakhomova, S. Xiao, A.G. Pakhomov, Manipulation of cell volume and membrane pore comparison following single cell permeabilization with 60- and 600-ns electric pulses, *BBA Biomembranes* 1808 (2011) 792–801.
- [15] R. Wayne, M. Tazawa, The actin cytoskeleton and polar water permeability in characean cells, *Protoplasma Suppl.* 2 (1988) 116–130.
- [16] A. Ismail, M. Riemann, P. Nick, The jasmonate pathway mediates salt tolerance in grapevines, *J. Exp. Bot.* 63 (2012) 2127–2139.
- [17] N. Kusaka, J. Maisch, P. Nick, K.I. Hayashi, H. Nozaki, Manipulation of intercellular auxin in a single cell by light with esterase-resistant caged auxins, *ChemBioChem* 10 (2009) 2195–2202.
- [18] F. Kumagai, A. Yoneda, T. Tomida, T. Sano, T. Nagata, S. Hasezawa, Fate of nascent microtubules organized at the M/G1 interface, as visualized by synchronized tobacco BY-2 cells stably expressing GFP-tubulin: time-sequence observations of the reorganization of cortical microtubules in living plant cells, *Plant Cell Physiol.* 42 (2001) 723–732.
- [19] F. Qiao, X. Chang, P. Nick, The cytoskeleton enhances gene expression in the response to the Harpin elicitor in grapevine, *J. Exp. Bot.* 61 (2010) 4021–4031.

- [20] L. Ebihara, J.E. Hall, R.C. MacDonald, T.J. McIntosh, S.A. Simon, Effect of benzyl alcohol on lipid bilayers. A comparison of bilayer systems, *Biophys. J.* 28 (1979) 185–196.
- [21] G.H. Lyman, H.D. Preisler, D. Papahadjopoulos, Membrane action of DMSO and other chemical inducers of Friend leukaemic cell differentiation, *Nature* 262 (1976) 361–363.
- [22] Z.M. Wei, R.J. Laby, C.H. Zumoff, D.W. Bauer, S.Y. He, A. Collmer, S.V. Beer, Harpin, elicitor of the hypersensitive response produced by the plant pathogen *Erwinia amylovora*, *Science* 257 (1992) 85–88.
- [23] X. Guan, G. Buchholz, P. Nick, The cytoskeleton is disrupted by the bacterial effector HrpZ, but not by the bacterial PAMP flg22, in tobacco BY-2 cells, *J. Exp. Bot.* 64 (2013) 1805–1816.
- [24] L. Taiz, E. Zeiger, *Plant Physiology*, third ed. Sinauer Associates, Sunderland, 2002.
- [25] M.D. Abramoff, P.J. Magalhaes, S.J. Ram, Image Processing with ImageJ, *Biophoton. Int.* 11 (2004) 36–42.
- [26] A.K. Azad, Y. Sawa, T. Ishikawa, H. Shibata, Phosphorylation of plasma membrane aquaporin regulates temperature-dependent opening of tulip petals, *Plant Cell Physiol.* 45 (2004) 608–617.
- [27] P.A. Janmey, D.A. Weitz, Dealing with mechanics: mechanisms of force transduction in cells, *Trends Biochem. Sci.* 29 (2004) 364–370.
- [28] A.W. Orr, B.P. Helmke, B.R. Blackman, M.A. Schwartz, Mechanisms of mechanotransduction, *Dev. Cell* 10 (2006) 11–20.
- [29] P. Nick, Mechanics of the cytoskeleton, in: P. Wojtaszek (Ed.), *Mechanical integration of plant cells and plants*, Springer, Berlin Heidelberg, 2011, pp. 53–90.
- [30] X. Chang, E. Heene, F. Qiao, P. Nick, The phytoalexin resveratrol regulates the initiation of hypersensitive cell death in *Vitis*, *PLoS One* 6 (2011) e26405, <http://dx.doi.org/10.1371/journal.pone.0026405>.
- [31] G. Komis, H. Quader, B. Galatis, P. Apostolakis, Microtubule-dependent protoplast volume regulation in plasmolysed root-tip cells of *Triticum turgidum*: involvement of phospholipase D, *New Phytol.* 11 (2006) 131–150.
- [32] Y. Hong, X. Pan, R. Welti, X. Wang, Phospholipase D $\alpha$ 3 is involved in the hyperosmotic response in *Arabidopsis*, *Plant Cell* 20 (2008) 803–816.
- [33] R. Pleskot, M. Potocký, P. Pejchar, J. Linek, R. Bezvoda, J. Martinec, O. Valentová, Z. Novotná, V. Žárský, Mutual regulation of plant phospholipase D and the actin cytoskeleton, *Plant J.* 62 (2010) 494–507.
- [34] J.C. Gardiner, J.D.I. Harper, N.D. Weerakoon, D.A. Collings, S. Ritchie, S. Gilroy, R.J. Cyr, J. Marc, A 90-kD phospholipase D from tobacco binds to microtubules and the plasma membrane, *Plant Cell* 13 (2001) 2143–2158.
- [35] P. Nick, Microtubules, signalling and abiotic stress, *Plant J.* (2013), <http://dx.doi.org/10.1111/tpj.12102>, (in press).
- [36] A. Akhmanova, M.O. Steinmetz, Tracking the ends: a dynamic protein network controls the fate of microtubule tips, *Nat. Rev. Mol. Cell Biol.* 9 (2008) 309–322.
- [37] S. Wang, J. Kurepa, T. Hashimoto, J.A. Smalle, Salt stress-induced disassembly of *Arabidopsis* cortical microtubule arrays involves 26S proteasome-dependent degradation of SPIRAL1, *Plant Cell* 23 (2011) 3412–3427.
- [38] T. Munnik, S.A. Arisz, T. de Vrije, A. Musgrave, G protein activation stimulates phospholipase D signaling in plants, *Plant Cell* 7 (1995) 2197–2210.
- [39] C. Testerink, T. Munnik, Molecular, cellular, and physiological responses to phosphatidic acid formation in plants, *J. Exp. Bot.* 62 (2011) 2349–2361.
- [40] J. Gardiner, D.A. Collings, J.D.I. Harper, J. Marc, The effects of the phospholipase D-antagonist 1-butanol on seedling development and microtubule organisation in *Arabidopsis*, *Plant Cell Physiol.* 44 (2003) 687–696.
- [41] P. Dhonukshe, A.M. Laxalt, J. Goedhart, T.W.J. Gadella, T. Munnik, Phospholipase D activation correlates with microtubule reorganization in living plant cells, *Plant Cell* 15 (2003) 2666–2679.
- [42] A. Hirase, T. Hamada, T.J. Itoh, T. Shimmen, S. Sonobe, *n*-Butanol induces depolymerization of microtubules *in vivo* and *in vitro*, *Plant Cell Physiol.* 47 (2006) 1004–1009.
- [43] N.T. Peters, K.O. Logan, A.C. Miller, D.L. Kropf, Phospholipase D signaling regulates microtubule organization in the fucoid alga *Silvetia compressa*, *Plant Cell Physiol.* 48 (2007) 1764–1774.
- [44] K. Raschke, Movements of Stomata, in: W. Haupt, M.E. Feinleb (Eds.), *Encyclopedia of plant physiology, Physiology of Movements*, Springer, Berlin, 1979, pp. 382–441.
- [45] B. Li, G. Liu, Y. Deng, M. Xie, Z. Feng, M. Sun, Y. Zhao, L. Liang, N. Ding, W. Jia, Excretion and folding of plasmalemma function to accommodate alterations in guard cell volume during stomatal closure in *Vicia faba L.*, *J. Exp. Bot.* 61 (2010) 3749–3758.
- [46] T. Meckel, A.C. Hurst, G. Thiel, U. Homann, Guard cells undergo constitutive and pressure-driven membrane turnover, *Protoplasma* 226 (2005) 23–29.
- [47] B. Li, M. Xie, M. Sun, W. Jia, How does plasmalemma surface area accommodate alterations in guard cell volume during stomatal closing? *Plant Signal. Behav.* 5 (2010) 1468–1469.
- [48] V. Sangwan, I. Foulds, J. Singh, R.S. Dhindsa, Cold-activation of *Brassica napus BN115* promoter is mediated by structural changes in membranes and cytoskeleton, and requires Ca<sup>2+</sup> influx, *Plant J.* 27 (2001) 1–12.
- [49] G. Komis, P. Apostolakis, B. Galatis, Altered patterns of tubulin polymerization in dividing leaf cells of *Chlorophyton comosum* after a hyperosmotic treatment, *New Phytol.* 149 (2001) 193–207.
- [50] M.J. Jaffe, A.C. Leopold, R.A. Staples, Thigmo responses in plants and fungi, *Am. J. Bot.* 89 (2002) 375–382.
- [51] U. Homann, Fusion and fission of plasma-membrane material accommodates for osmotically induced changes in the surface area of guard-cell protoplasts, *Planta* 206 (1998) 329–333.
- [52] J. Wolfe, M.F. Dowgert, P.L. Steponkus, Dynamics of membrane exchange of the plasma membrane and the lysis of isolated protoplasts during rapid expansions in area, *J. Membr. Biol.* 86 (1985) 127–138.
- [53] A.A. Gurtovenko, J. Anwar, Modulating the structure and properties of cell membranes: the molecular mechanism of action of dimethyl sulfoxide, *J. Phys. Chem. B* 111 (2007) 10453–10460.
- [54] Q.Y. Wang, P. Nick, The auxin response of actin is altered in the rice mutant *Yin-Yang*, *Protoplasma* 204 (1998) 22–33.